Geochemical Perspectives Letters

Silver isotope fractionation by chemical diffusion in granitic melt

S. Li[1], L. Zhang[1], Y. Fang[1], H. Ni[1,2,3], F. Huang[1,2,3*]

https://doi.org/10.7185/geochemlet.2552

Abstract

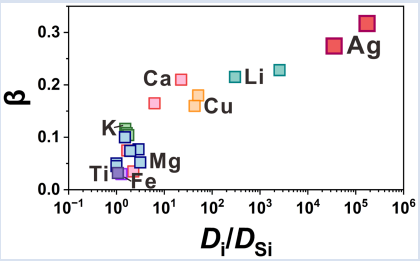

We report the first study of silver (Ag) isotope fractionation during diffusion in anhydrous granitic melts using diffusion couple experiments. The mass dependence of the diffusion coefficients of the Ag isotopes can be described by $D_{^{109}Ag}/D_{^{107}Ag} = (107/109)^{\beta}$. In this study, we performed piston-cylinder experiments to constrain the β-factor for Ag isotopic fractionation by diffusion in anhydrous granitic melts. By regression and error estimation of the diffusive isotope profiles, we obtained β-values of 0.317 ± 0.036 and 0.274 ± 0.016 for the two diffusion experiments. These β-values are the largest in metal stable isotopes reported for silicate melts, reflecting rapid diffusion and minimal interaction of Ag^{+} with the melt network. A theoretical model was established based on experimental data, predicting significant diffusive Ag isotope fractionation (>6 ‰) during granitic magma ascent and fluid exsolution. The modelling results suggest that Ag isotopes can be used to trace silver migration, magma mixing and mineralisation processes.

Received 1 July 2025 | Accepted 3 November 2025 | Published 22 December 2025

Introduction

Silver (Ag), a moderately volatile transition element known for its thiophilicity and polarisability, is commonly found in nature as sulfides, sulfosalts and natural silver. Ag is also a precious metal of great economic and strategic importance due to its high electrical and thermal conductivity. Ag has a relatively low content in various geological samples and is heterogeneously distributed. The Ag content in CI chondrites is about 208 ng/g, about 7.1 µg/g in the solar system, 0.05 µg/g on BSE and 0.15 µg/g in the core (McDonough and Sun, 1995; McDonough, 2003).

Ag has two stable isotopes: ^{107}Ag (51.839 %) and ^{109}Ag (48.161 %) (Rosman and Taylor, 1998). Due to its unique geochemical properties, Ag isotopes have significant potential in a variety of areas. As a moderately volatile element, stable Ag isotopes are expected to be an emerging geochemical tracer. Important application aspects are: 1) Ag may have mainly entered the Earth's core during the early stages of Earth's evolution, and Ag isotopes can help us understand the core formation process (Theis *et al.*, 2013); 2) Ag is highly chalcophile, and its isotopes can be used to constrain the crust–mantle interactions, particularly material transfer between the mantle and the crust (Righter *et al.*, 2020); 3) Experimental and theoretical findings indicate that Ag has a propensity to enrich light isotopes in the reduced phase and heavy isotopes in the oxidised phase (Mathur *et al.*, 2018). Therefore, Ag isotopes can preserve information on oxygen fugacity and temperature changes during magmatism and mineralisation (Voisey *et al.*, 2019; Wang *et al.*, 2022).

Diffusion plays a key role in the material transport mechanisms within magmatic systems, with the potential to induce significant isotopic fractionation. Experimental studies have shown that Ag diffuses rapidly, resulting in efficient Ag transfer from the silicate melt to the hydrothermal and sulfide fluid, which is beneficial for Ag mineralisation (Zhang *et al.*, 2021). Although there are currently no data of natural samples that demonstrate significant Ag isotope fractionation through diffusion, understanding the diffusion properties of Ag isotopes could help to explain the Ag transport and enrichment processes in magmatic and hydrothermal activities. The relative diffusivities of the two isotopes can be expressed as follows: $D_1/D_2 = (m_2/m_1)^{\beta}$, where D_1 and D_2 are isotopic diffusivities, and m_1 and m_2 are atomic masses (Richter *et al.*, 1999). In order to quantify the magnitude of Ag isotope fractionation by chemical diffusion, it is necessary to constrain the β-factor, which is an empirical value ranging from 0 to 0.5. However, there is still no experimental study on diffusive fractionation of Ag isotopes in silicate melts. In this study, we performed piston-cylinder experiments to determine β-factors for Ag isotope fractionation by diffusion in granitic melts.

Experimental and Analytical Methods

All experiments and analyses were carried out at the University of Science and Technology of China. For the diffusion experiments, two types of anhydrous glasses were prepared. The two glasses have similar major element compositions but distinct Ag concentrations (25–36 µg/g *vs.* 190–310 µg/g). The glass utilised in both experiments exhibited an Ag content variation of

1. State Key Laboratory of Lithospheric and Environmental Coevolution, USTC, Hefei 230026, China
2. CAS Center for Excellence in Comparative Planetology, USTC, Hefei 230026, Anhui, China
3. Institute of Deep Space Sciences, Deep Space Exploration Laboratory, Hefei, China
* Corresponding author (email: fhuang@ustc.edu.cn)

less than 5 %, a value that can be regarded as homogeneous. Maintaining only the Ag content as the variable can eliminate interference from variations in other compositions and ensure that the Ag concentration gradient is the only driving force for isotope fractionation. Consequently, the contribution of diffusion to isotopic fractionation can be quantified, and the Ag diffusion coefficient and β-factor can be accurately determined. The two glass cylinders were double polished and fit closely into a graphite capsule with an outer diameter of 4.6 mm; then, the graphite capsule was welded shut in a Pt capsule. The capsule was placed inside a ¾″ talc-pyrex-graphite-MgO assembly. Both experiments were conducted at 1 GPa, with LSTAg2 at 1473 K for 9.49 minutes and LSTAg3 at 1273 K for 57.69 minutes. Rapid quenching was applied by power shutdown. Because the diffusion took place within one hour, isotope fractionation driven by thermal diffusion is not further considered (Huang *et al.*, 2009, 2010). Detailed sample description and experimental methods are provided in the Supplementary Information.

After the experiments, the first step was to cut samples longitudinally in half along their centre using a diamond saw. One half of the sample was mounted inside an epoxy resin and then polished for EPMA and LA-ICP-MS analysis. The other half was etched at the USTC Center for Micro- and Nanoscale Research and Fabrication using a laser ultra-precision processing system, where the glass samples were cut into seven pieces, each 200–300 um wide and then removed under a microscope using tweezers (Fig. 1). This method allows precise determination of the location of each glass piece.

Chemical digestion and purification processes for Ag isotope analysis were performed in a metal-free clean laboratory. Given the knowledge of the elements contained in the diffusion experimental samples, using a single column of cation resin (AG50 W-X8) was sufficient to completely separate Ag. The resin was cleaned with 6 N HNO_3 (30 mL), followed by a final rinse with Milli-Q H_2O (5 mL). The resin was then filled in Savillex microcolumns. The purification process used 6 N HNO_3 throughout to separate Ag and other elements. The overall yield of Ag from the chemical process was >95 %. Ag solutions were diluted to 5 or 10 ng/g for analysis.

Ag isotope ratios were analysed using a Neptune Plus MC-ICP–MS. The isotope composition is expressed as follows:

$$\delta^{109}\mathrm{Ag} = \left(\frac{(^{109}\mathrm{Ag}/^{107}\mathrm{Ag})_{\mathrm{sample}}}{(^{109}\mathrm{Ag}/^{107}\mathrm{Ag})_{\mathrm{standard}}} - 1\right) \times 1000‰ \qquad \text{Eq. 1}$$

Each sample was measured more than three times. A bracketing standard (NIST SRM978a) was used during the analysis and AAS-Ag solution was used to monitor instrumental stability. We made two synthetic Ag standards (LOW-Ag and HIGH-Ag), consisting of different Ag contents with other matrix elements to verify the reliability of Ag isotope measurement. The standards (LOW-Ag and HIGH-Ag) yielded δ^{109}Ag values of $+0.05 \pm 0.02$ ‰ and $+0.02 \pm 0.02$ ‰, respectively, which is consistent with the recommended value (0.00 ‰) within error. All analytical conditions are provided in the Supplementary Information.

Ag Diffusion Coefficients in Anhydrous Granitic Melt

The major element composition of the glass in the LSTAg2 experiment is shown in Figure S-2, with small variations (less than 10 % relative variation) in major elements. This observation indicates that the major elements are homogeneous, suggesting that diffusion is not affected by melt composition during the experiments, and that the concentration gradient of Ag is the sole driver of diffusion occurrence. The Ag concentration profiles are fitted by the analytical solution to a one-dimensional diffusion couple (Crank, 1975):

$$C = \frac{C_L + C_R}{2} + \frac{C_R - C_L}{2}\,\mathrm{erf}\left(\frac{x - x_0}{2\sqrt{Dt}}\right) \qquad \text{Eq. 2}$$

where C_L and C_R are the initial Ag concentrations of the low-Ag and high-Ag glasses at the flat regions, respectively, x_0 is the position of the interface, D is Ag diffusivity and t is time. Four parameters (C_L, C_R, x_0, D) were simultaneously optimised through non-linear least squares fitting with initial values set based on data characteristics and the final results were evaluated for error using the covariance matrix. The fits for the two experiments were: for LSTAg3 (1273 K), $C_L = 25.8$ μg/g, $C_R = 190.9$ μg/g, $x_0 = 183.7$ μm, $D = 33.0 \pm 1.7$ μm^2/s; and for LSTAg2 (1473 K), $C_L = 35.1$ μg/g, $C_R = 308.7$ μg/g, $x_0 = -84.9$ μm, $D = 125.8 \pm 6.2$ μm^2/s. The diffusion coefficient agrees well with both the

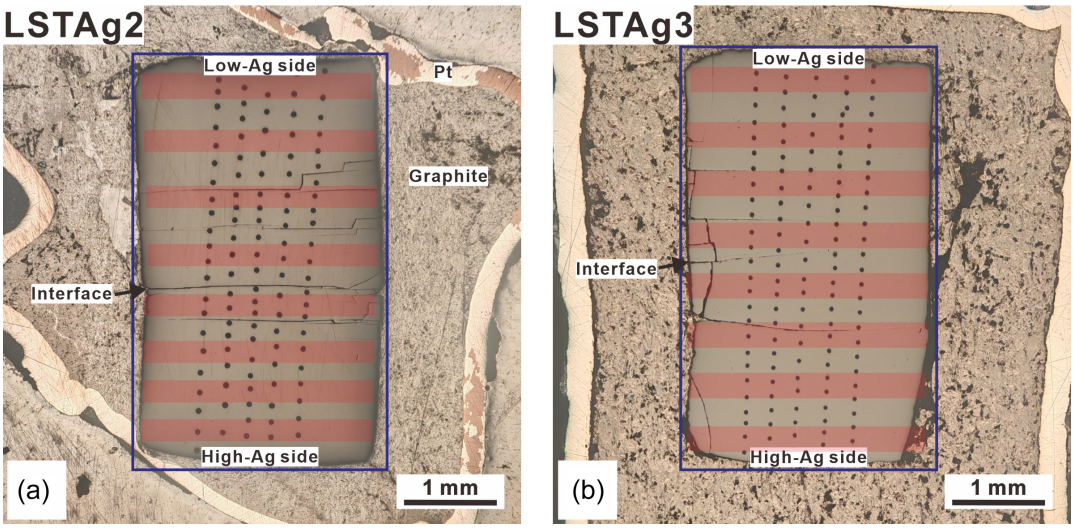

Figure 1 **(a)** Reflected light photo of LSTAg2. **(b)** Reflected light photo of LSTAg3. The black spots indicate the position of laser ablation pits. The five lines from left to right are designated as Line A to Line E. The blue rectangles represent the first etching using laser ultra-precision processing system. The red rectangles show location information sampled for Ag isotopic measurements.

calculated results developed by Mungall (2002) and the empirical model for Ag diffusion reported by Zhang *et al.* (2021).

Ag Isotope Fractionation in Anhydrous Granitic Melt

The measured Ag isotopic composition profiles for both experiments show significant δ^{109}Ag variation, from 5.21 ± 0.13 ‰ to 2.10 ± 0.05 ‰ (Table S-3). For the two diffusion-couple experiments, the δ^{109}Ag measured at the high concentration end was 4.28 ± 0.07 ‰ (LSTAg2) and 4.31 ± 0.02 ‰ (LSTAg3), which are in general agreement with the independent measurements of the HIGH-Ag initial glass (~4.14 ± 0.02 ‰). The δ^{109}Ag measured at the low end was 5.21 ± 0.13 ‰ (LSTAg2) and 4.37 ± 0.11 ‰ (LSTAg3), while the LOW-Ag initial glass ~4.74 ± 0.03 ‰. For LSTAg2, the LOW-Ag glass (4.74 ± 0.03 ‰) can be used as the low concentration end (see Fig. 2). The relative diffusivities of ^{107}Ag and ^{109}Ag are expressed by β in the equation:

$$\frac{D_{^{109}\mathrm{Ag}}}{D_{^{107}\mathrm{Ag}}} = \left(\frac{107}{109}\right)^{\beta} \qquad \text{Eq. 3}$$

where $D_{^{107}\mathrm{Ag}}$ and $D_{^{109}\mathrm{Ag}}$ are the diffusivities of ^{107}Ag and ^{109}Ag, respectively. β is constrained by regression using nonlinear least squares fitting, and the standard error of β was calculated using the covariance matrix. This was to find the value of β that best matches the model predictions to the measured data with rigorous error analysis. The fits of the β-factor obtained by this method were 0.274 ± 0.016 (2σ) for LSTAg2 and 0.317 ± 0.036 (2σ) for LSTAg3, respectively (Table S-2). The calculated Ag fractionation profiles are highly consistent with the measured data, thereby confirming the hypothesis that ^{107}Ag and ^{109}Ag diffuse at different rates. Experimental determination of β-factors has been conducted for seven metal elements (Li, Ca, Mg, Fe, K, Cu and Ti), within the range of 0.030 to 0.228 (Richter *et al.*, 2003, 2008, 2009b; Watkins *et al.*, 2009, 2011; Chopra *et al.*, 2012; Holycross *et al.*, 2018; Zhang, 2022; Ni and Shahar, 2023; Zhang and Bai, 2025; Zhou *et al.*, 2025). Among these elements, Ag has the highest β-factor, with its diffusion coefficient of Ag in granite melts only slightly lower than that of Li. The high β-factor for Ag can be explained by its unique geochemical properties. Calculations

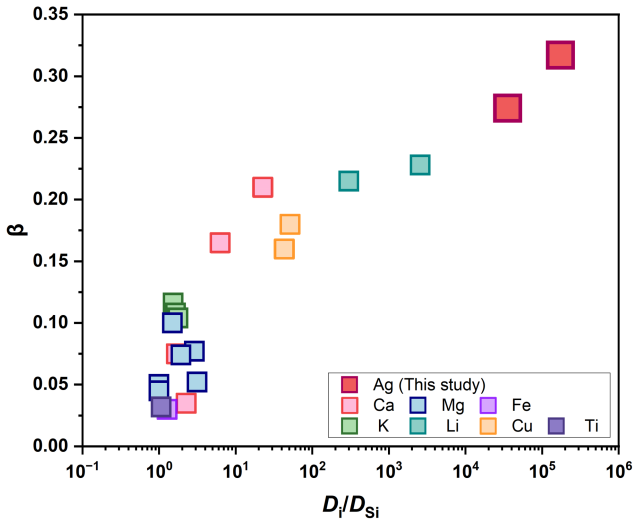

Figure 3 The relationship between experimentally determined β_i-factor and D_i/D_{Si} for eight metal elements. Data are from: Ca (Richter *et al.*, 2003; Watkins *et al.*, 2009, 2011), Mg (Richter *et al.*, 2008; Watkins *et al.*, 2011; Chopra *et al.*, 2012; Zhang and Bai, 2025), Fe (Richter *et al.*, 2009b), K (Zhang, 2022), Li (Richter *et al.*, 2003; Holycross *et al.*, 2018), Cu (Ni and Shahar, 2023), Ti (Zhou *et al.*, 2025) and Ag (this work).

using silicon self-diffusion data from Zhang and Gan (2022) yielded D_{Ag}/D_{Si} of 35,000 and 170,000 for the two experiments (Fig. 3). This suggests that β increases with D_i/D_{Si} (where i is the element of interest), supporting the correlation between the β-factor and Si-normalised diffusivity as posited in previous studies (Watkins *et al.*, 2017; Holycross *et al.*, 2018). As a monovalent cation with a large ionic radius and low field strength, Ag^+ interacts minimally with the silicate melt network due to its fast diffusion rate, resulting in diffusion behaviour that is almost independent, making it more easy moving within the melt network. Consequently, the mass-related dependence of diffusivity is strongly affected by the differences in relative mass among isotopes. This trend is largely consistent with the observations in this study, which validates the correlation between β and D_i/D_{Si}.

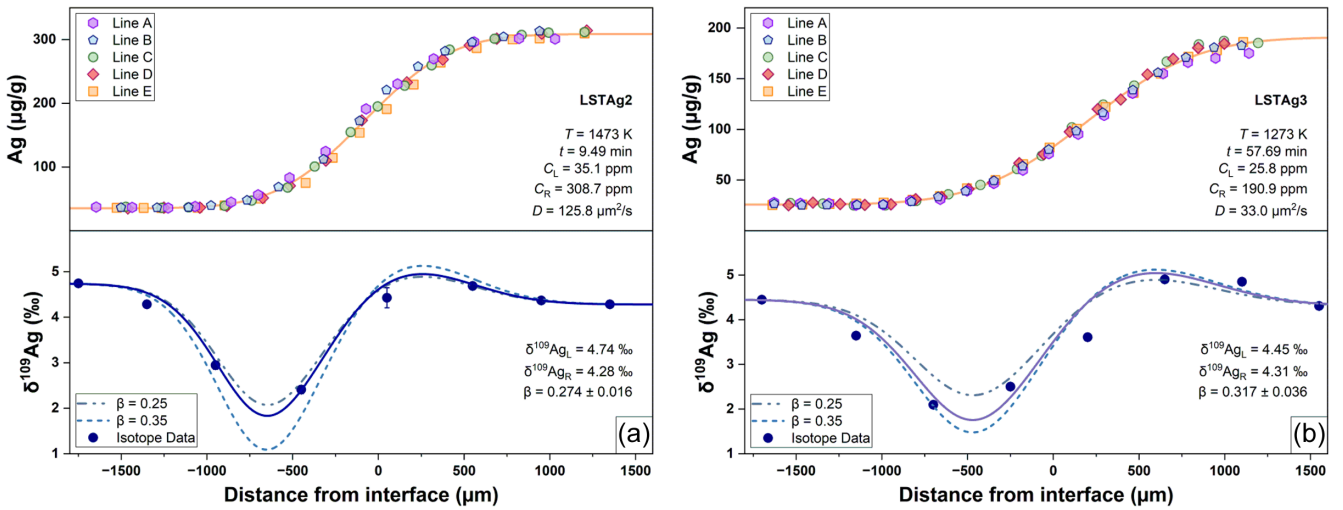

Figure 2 Ag concentration measured by LA-ICP-MS and δ^{109}Ag measured by MC-ICP-MS. The five lines are represented by Line A to Line E longitudinally through the sample, from left to right. The concentration profiles of LSTAg2 and LSTAg3 were fitted using finite diffusion couple solutions, assuming a constant effective binary diffusivity (EBD). Orange line shows error function fits. A comparison was made between the Ag fractionation data for two experiments and profiles calculated using various β-factors. Blue line represents the best fit of δ^{109}Ag profile (β = 0.274 ± 0.016 for LSTAg2 and 0.317 ± 0.036 for LSTAg3).

In the diffusion process, light isotopes consistently diffuse faster than heavy isotopes, leading to comparative light isotope enrichment at the low concentration end (Richter *et al.*, 2008, 2009a). Following the modelling in Richter *et al.* (2003), which estimated diffusive isotope fractionation as a function of β-factor and concentration difference, this study combines Ag isotope experimental data with model predictions. Figure S-3 demonstrates the relationship between isotope fractionation by diffusion and the diffusion coefficients ratio of the two isotopes (D_1/D_2) as well as the elemental concentration ratio (C_1/C_2). The modelling results indicate that significant isotope fractionation can occur with a sufficiently large elemental concentration difference and a notable β-value. This is crucial for evaluating the applicability of experimental results to natural silicate melts. The theoretical framework in Figure S-3 establishes a set of geochemical methodologies for identifying diffusion processes through isotope fractionation, which can be used to understand and predict Ag isotope variations in natural samples. Given the rapid advance in metal stable isotope analytical techniques, Ag isotopic compositions of these metal elements can shed more light on the diffusion processes and kinetic conditions in magmatic systems and provide rich information for understanding the chemical evolution and physical processes of magmas. Subsequent studies that integrate Ag isotopes with other geochemical tracers (*e.g.*, Cu, S isotopes) will further delineate the relative significance of diffusion as compared to other geochemical processes in magmatic–hydrothermal systems.

Modelling Ag Isotope Fractionation in Hydrothermal-Magmatic Systems

To demonstrate the geological significance of the Ag isotope data, we construct a numerical model of fluid exsolution distribution and Ag diffusive isotope fractionation during granitic magma ascent. The initial granitic melt undergoes fluid desorption driven by decompression (Fig. 4). Ag can be partitioned between the fluid and residual melt. In accordance with the principle of conservation of mass, Ag content in melt can be deduced as:

$$C^0_{Ag}M^0_m = C^m_{Ag}M_m + C^b_{Ag}M_b \quad \text{Eq. 4}$$

The experimentally determined brine/melt partition coefficient of Ag ($\frac{C^b_{Ag}}{C^m_{Ag}}$) is set to 413 (Simon *et al.*, 2008), typically with fluid mass fractions of ~5–10 %. The UCC silver content is approximately 50 ng/g (Taylor and McLennan, 1985), and a concentration gradient can be formed at the melt interface due to loss of Ag into the fluid. Assuming the D_{Ag} is 125.8 μm^2/s at 1 GPa and 1473 K and the β is 0.3 value as obtained in this study, the diffusion profiles and isotope profiles for different time sequences can be calculated as shown in Figures 4 and S-4. The model predicts that the diffusive fractionation for Ag isotopes could be greater than 6 ‰, suggesting that Ag isotopes can be a useful tracer for Ag transport in granitic magmatism.

In summary, the results of the diffusion experiments show rapid Ag diffusion and significant Ag isotope fractionation. The experimental determination of Ag isotope fractionation during diffusion provides a quantitative framework for interpreting Ag isotopic variations in natural systems. The remarkably elevated β-factor of Ag isotopes serves to substantiate the notion that kinetic processes have the capacity to engender substantial diffusive Ag isotope fractionation during the magmatic and hydrothermal processes, likely involving magma mixing, fluid exsolution and mineral segregation. This is essential for using the experimentally measured β_{Ag} to model the kinetic Ag isotope fractionation in natural systems to understand how Ag is transferred in the Earth's system.

Acknowledgements

This study was financially supported by the National Natural Science Foundation of China (42330101). We are grateful to

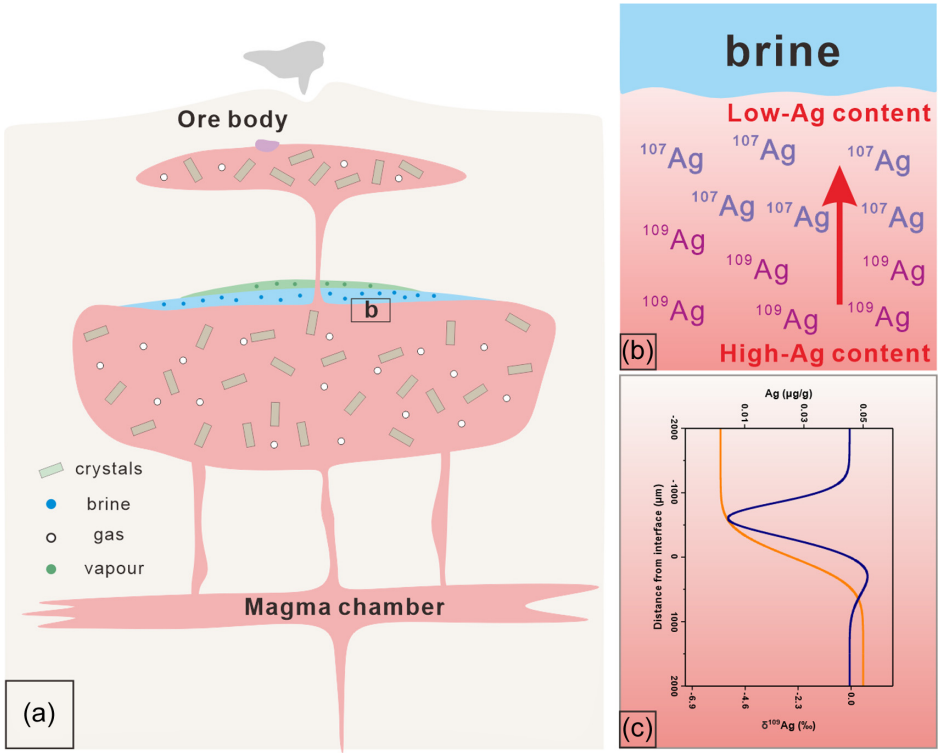

Figure 4 Schematic model of magma ascent and decompression process.

Editor Raúl Fonseca, Reviewer Megan Holycross, and an anonymous reviewer for their constructive comments.

Editor: Raul O.C. Fonseca

Additional Information

Supplementary Information accompanies this letter at https://www.geochemicalperspectivesletters.org/article2552.

Cite this letter as: Li, S., Zhang, L., Fang, Y., Ni, H., Huang, F. (2025) Silver isotope fractionation by chemical diffusion in granitic melt. *Geochem. Persp. Let.* 38, 29–33. https://doi.org/10.7185/geochemlet.2552

References

Chopra, R., Richter, F.M., Watson, E.B., Scullard, C.R. (2012) Magnesium isotope fractionation by chemical diffusion in natural settings and in laboratory analogues. *Geochimica et Cosmochimica Acta* 88, 1–18. https://doi.org/10.1016/j.gca.2012.03.039

Crank, J. (1975) *The Mathematics of Diffusion*. Second Edition, Oxford University Press, Oxford.

Holycross, M.E., Watson, E.B., Richter, F.M., Villeneuve, J. (2018) Diffusive fractionation of Li isotopes in wet, highly silicic melts. *Geochemical Perspectives Letters* 6, 39–42. https://doi.org/10.7185/geochemlet.1807

Huang, F., Lundstrom, C.C., Glessner, J., Ianno, A., Boudreau, A., Li, J., Ferré, E.C., Marshak, S., DeFrates, J. (2009) Chemical and isotopic fractionation of wet andesite in a temperature gradient: Experiments and models suggesting a new mechanism of magma differentiation. *Geochimica et Cosmochimica Acta* 73, 729–749. https://doi.org/10.1016/j.gca.2008.11.012

Huang, F., Chakraborty, P., Lundstrom, C.C., Holmden, C., Glessner, J.J.G., Kieffer, S.W., Lesher, C.E. (2010) Isotope fractionation in silicate melts by thermal diffusion. *Nature* 464, 396–400. https://doi.org/10.1038/nature08840

Mathur, R., Arribas, A., Megaw, P., Wilson, M., Stroup, S., Meyer-Arrivillaga, D., Arribas, I. (2018) Fractionation of silver isotopes in native silver explained by redox reactions. *Geochimica et Cosmochimica Acta* 224, 313–326. https://doi.org/10.1016/j.gca.2018.01.011

McDonough, W.F. (2003) 2.15 - Compositional model for the Earth's core. In: Holland, H.D., Turekian, K.K. (Eds.) *Treatise on Geochemistry*. First Edition, Elsevier, Amsterdam, 547–568. https://doi.org/10.1016/B0-08-043751-6/02015-6

McDonough, W.F., Sun, S.-s. (1995) The composition of the Earth. *Chemical Geology* 120, 223–253. https://doi.org/10.1016/0009-2541(94)00140-4

Mungall, J.E. (2002) Empirical models relating viscosity and tracer diffusion in magmatic silicate melts. *Geochimica et Cosmochimica Acta* 66, 125–143. https://doi.org/10.1016/S0016-7037(01)00736-0

Ni, P., Shahar, A. (2023) Copper isotope fractionation by diffusion in a basaltic melt. *Earth and Planetary Science Letters* 624, 118459. https://doi.org/10.1016/j.epsl.2023.118459

Richter, F.M., Liang, Y., Davis, A.M. (1999) Isotope fractionation by diffusion in molten oxides. *Geochimica et Cosmochimica Acta* 63, 2853–2861. https://doi.org/10.1016/S0016-7037(99)00164-7

Richter, F.M., Davis, A.M., DePaolo, D.J., Watson, E.B. (2003) Isotope fractionation by chemical diffusion between molten basalt and rhyolite. *Geochimica et Cosmochimica Acta* 67, 3905–3923. https://doi.org/10.1016/S0016-7037(03)00174-1

Richter, F.M., Watson, E.B., Mendybaev, R.A., Teng, F.-Z., Janney, P.E. (2008) Magnesium isotope fractionation in silicate melts by chemical and thermal diffusion. *Geochimica et Cosmochimica Acta* 72, 206–220. https://doi.org/10.1016/j.gca.2007.10.016

Richter, F.M., Dauphas, N., Teng, F.-Z. (2009a) Non-traditional fractionation of non-traditional isotopes: Evaporation, chemical diffusion and Soret diffusion. *Chemical Geology* 258, 92–103. https://doi.org/10.1016/j.chemgeo.2008.06.011

Richter, F.M., Watson, E.B., Mendybaev, R., Dauphas, N., Georg, B., Watkins, J., Valley, J. (2009b) Isotopic fractionation of the major elements of molten basalt by chemical and thermal diffusion. *Geochimica et Cosmochimica Acta* 73, 4250–4263. https://doi.org/10.1016/j.gca.2009.04.011

Righter, K., Schönbächler, M., Pando, K., Rowland II, R., Righter, M., Lapen, T. (2020) Ag isotopic and chalcophile element evolution of the terrestrial and martian mantles during accretion: New constraints from Bi and Ag metal-silicate partitioning. *Earth and Planetary Science Letters* 552, 116590. https://doi.org/10.1016/j.epsl.2020.116590

Rosman, K.J.R., Taylor, P.D.P. (1998) Isotopic compositions of the elements 1997 (Technical Report). *Pure and Applied Chemistry* 70, 217–235. https://doi.org/10.1351/pac199870010217

Simon, A.C., Pettke, T., Candela, P.A., Piccoli, P.M. (2008) The partitioning behavior of silver in a vapor–brine–rhyolite melt assemblage. *Geochimica et Cosmochimica Acta* 72, 1638–1659. https://doi.org/10.1016/j.gca.2008.01.003

Taylor, S.R., McLennan, S.M. (1985) *The Continental Crust: Its Composition and Evolution*. Blackwell Scientific Publications, Oxford.

Theis, K.J., Schönbächler, M., Benedix, G.K., Rehkämper, M., Andreasen, R., Davies, C. (2013) Palladium–silver chronology of IAB iron meteorites. *Earth and Planetary Science Letters* 361, 402–411. https://doi.org/10.1016/j.epsl.2012.11.004

Voisey, C.R., Maas, R., Tomkins, A.G., Brauns, M., Brügmann, G. (2019) Extreme Silver Isotope Variation in Orogenic Gold Systems Implies Multistaged Metal Remobilization During Ore Genesis. *Economic Geology* 114, 233–242. https://doi.org/10.5382/econgeo.2019.4629

Wang, J.-L., Wei, H.-Z., Williams-Jones, A.E., Dong, G., Zhu, Y.-F., Jiang, S.-Y., Ma, J., Hohl, S.V., Liu, X., Li, Y.-C., Lu, J.-J. (2022) Silver isotope fractionation in ore-forming hydrothermal systems. *Geochimica et Cosmochimica Acta* 322, 24–42. https://doi.org/10.1016/j.gca.2022.01.024

Watkins, J.M., DePaolo, D.J., Huber, C., Ryerson, F.J. (2009) Liquid composition-dependence of calcium isotope fractionation during diffusion in molten silicates. *Geochimica et Cosmochimica Acta* 73, 7341–7359. https://doi.org/10.1016/j.gca.2009.09.004

Watkins, J.M., DePaolo, D.J., Ryerson, F.J., Peterson, B.T. (2011) Influence of liquid structure on diffusive isotope separation in molten silicates and aqueous solutions. *Geochimica et Cosmochimica Acta* 75, 3103–3118. https://doi.org/10.1016/j.gca.2011.03.002

Watkins, J.M., DePaolo, D.J., Watson, E.B. (2017) Kinetic Fractionation of Non-Traditional Stable Isotopes by Diffusion and Crystal Growth Reactions. *Reviews in Mineralogy and Geochemistry* 82, 85–125. https://doi.org/10.2138/rmg.2017.82.4

Zhang, L., Guo, X., Li, W.-C., Ding, J., Bai, B., Ni, H. (2021) Rapid Ag diffusion in granitic melt: Implications for Ag mineralization and melt inclusion record. *Geochimica et Cosmochimica Acta* 310, 47–60. https://doi.org/10.1016/j.gca.2021.07.008

Zhang, Y. (2022) Diffusive fractionation of K isotopes in molten basalts. *Earth and Planetary Science Letters* 581, 117405. https://doi.org/10.1016/j.epsl.2022.117405

Zhang, Y., Gan, T. (2022) Diffusion in Melts and Magmas. *Reviews in Mineralogy and Geochemistry* 87, 283–337. https://doi.org/10.2138/rmg.2022.87.07

Zhang, Y., Bai, B. (2025) Diffusive Mg isotope fractionation in silicate melts during mineral dissolution. *Chemical Geology* 681, 122720. https://doi.org/10.1016/j.chemgeo.2025.122720

Zhou, S., Zhang, Y., Kita, N.T. (2025) Diffusive titanium isotope fractionation in silicate melts. *Earth and Planetary Science Letters* 651, 119176. https://doi.org/10.1016/j.epsl.2024.119176